Central memory self/tumor-reactive CD8$^+$ T cells confer superior antitumor immunity compared with effector memory T cells

Christopher A. Klebanoff*†‡, Luca Gattinoni†‡, Parizad Torabi-Parizi*§, Keith Kerstann†, Adela R. Cardones¶, Steven E. Finkelstein†, Douglas C. Palmer†, Paul A. Antony†, Sam T. Hwang¶, Steven A. Rosenberg†, Thomas A. Waldmann‖, and Nicholas P. Restifo†**

*Howard Hughes Medical Institute, National Institutes of Health Research Scholars Program, Bethesda, MD 20814; and Branches of †Surgery, ¶Dermatology, and ‖Metabolism, National Cancer Institute, and §Laboratory of Immunology, National Institute of Allergy and Infectious Diseases, National Institutes of Health, Bethesda, MD 20892

Contributed by Thomas A. Waldmann, May 6, 2005

Central memory CD8$^+$ T cells (T_{CM}) and effector memory CD8$^+$ T cells (T_{EM}) are found in humans and mice; however, their relative contributions to host immunity have only recently been examined *in vivo*. Further, the ability of T_{CM} to treat an established tumor or infection has yet to be evaluated. To address the therapeutic potential of different tumor-reactive CD8$^+$ T cell memory subsets, we used an established model for the *in vitro* generation of T_{CM} and T_{EM} by using IL-15 and IL-2, respectively. Adoptively transferred T_{CM} exhibited a potent *in vivo* recall response when combined with tumor-antigen vaccination and exogenous IL-2, leading to the eradication of large established tumors. By contrast, T_{EM} were far less effective on a per-cell basis. Microarray analysis revealed that the signature of highly *in vivo* effective antitumor T cells included the overexpression of genes responsible for trafficking to secondary lymphoid tissues. This gene expression profile correctly predicted the *in vitro* and *in vivo* lymphoid-homing attributes of tumor-reactive T cells. Furthermore, we found that homing to secondary lymphoid tissue is required for optimal tumor treatment. Our findings indicated that highly *in vivo* effective antitumor T cells were those that initially targeted secondary lymphoid tissue, rather than tumor sites, as had previously been postulated. Thus, tumor-reactive CD8$^+$ T cell populations with the phenotypic and functional attributes of T_{CM} may be superior to T_{EM}/effector T cells for adoptive immunotherapies using concomitant tumor-antigen vaccination.

IL-2 | IL-15 | | homing | immunotherapy | vaccine

Adoptive cancer immunotherapy, the infusion of tumor-reactive T cells to patients, represents a promising approach for the treatment of advanced metastatic disease (1, 2). To date, cell types with effector T cell (T_{EFF}) and effector memory CD8$^+$ T cell (T_{EM}) phenotype and function have been the cells targeted for transfer because of their strong lytic capacity and release of high levels of IFN-γ (3, 4). Although transfer of polyclonal tumor-reactive T_{EFF} can cause an objective response rate approaching 50% (5), there are reasons to believe that transfer of cells with memory properties, including a heightened recall response and the ability to undergo self-renewal, may be superior mediators of an antitumor response (6, 7).

The T cell memory compartment can be subdivided into two populations, central memory CD8$^+$ T cells (T_{CM}) and T_{EM}, on the basis of phenotypic markers, functional attributes, and migratory properties (7). CD62L and CCR7, two surface molecules necessary for cellular extravasation in high endothelial venules, are constitutively expressed by T_{CM}, whereas these markers are significantly down-regulated on T_{EM}. T_{CM} have been shown to be superior to T_{EM} in conferring protective immunity against viral or bacterial challenge (8, 9). However, the extent to which these results can be generalized has been questioned (10), and the potential of T_{CM} to treat an established infection or cancer has not been evaluated.

To assess the *in vivo* role of different CD8$^+$ T cell memory subsets, we used an established *in vitro* culture system by using IL-15 and IL-2 to generate T_{CM} and T_{EM}, respectively (8, 11–13). To generate tumor-reactive CD8$^+$ T cells, we used cells from pmel-1 T cell receptor transgenic mice. Pmel-1 mice have CD8$^+$ T cells that have specificity for a D^b-restricted epitope corresponding to amino acid positions 25–33 of the nonmutated self/tumor antigen (Ag) gp100 (14). The two cell subtypes were verified by using global analysis of gene expression as well as phenotypic and functional characteristics. We found that adoptive cell transfer (ACT) of self/tumor-reactive CD8$^+$ T_{CM} was a superior mediator of tumor treatment compared with T_{EM}.

Materials and Methods

Mice and Tumor Lines. Pmel-1 T cell receptor transgenic mice expressing CD8$^+$ T cells with specificity for a D^b-restricted epitope from the nonmutated self/tumor Ag $gp100_{25–33}$ (14) were crossed with C57BL/6-thy1.1 transgenic and C57BL/6-Sell$^{-/-}$ mice (both from The Jackson Laboratory) to derive pmel-thy1.1 (deposited at The Jackson Laboratory, www.jax.org) and pmel-CD62L$^{-/-}$ (pmel CD62L knockout) mice (26), respectively. Female C57BL/6 and B6.129S2-Lta^{tm1Dch}/J (both from The Jackson Laboratory) and β_2-microglobulin (β_2M)-deficient ($\beta_2M^{-/-}$) mice (Taconic Farms) were used as recipients in ACT experiments. B16 (H-2^b), a spontaneous gp100$^+$ murine melanoma, has been described (14). Experiments were conducted with the approval of the National Cancer Institute Animal Use and Care Committee.

T_{CM} and T_{EM} Generation and Adoptive Immunotherapy. Pmel-1 splenocytes were isolated and cultured in the presence of 1 μM human $gp100_{25–33}$ ($hgp100_{25–33}$) and complete medium containing 10 ng/ml of either recombinant human IL-2 (Chiron) to generate pmel T_{EM} or recombinant human IL-15 (PeproTech, Rocky Hill, NJ) to generate pmel T_{CM} (12). Mice ($n = 5$) were injected s.c. with 2–5 $\times$ 10^5 B16-F10 melanoma cells. Nine days later, mice were treated with i.v. ACT of pmel T_{CM} or T_{EM}. Where specified, transient lymphopenia was induced by sublethal irradiation (500 cGy) of tumor-bearing mice on the day of treatment. Vaccination was achieved with 2 $\times$ 10^7 plaque-forming units of a recombinant fowlpox virus encoding hgp100

Abbreviations: Ag, antigen; hgp100, human gp100; rFPhgp100, recombinant fowlpox virus encoding hgp100; T_{EM}, effector memory CD8$^+$ T cells; T_{CM}, central memory CD8$^+$ T cells; LN, lymph node; ACT, adoptive cell transfer; DC, dendritic cell; CFSE, carboxyfluorescein diacetate succinimidyl ester; LTα, lymphotoxin-α; β_2M, β_2-microglobulin; BM, bone marrow.

‡C.A.K. and L.G. contributed equally to this work.

**To whom correspondence should be addressed. E-mail: restifo@nih.gov.

IMMUNOLOGY

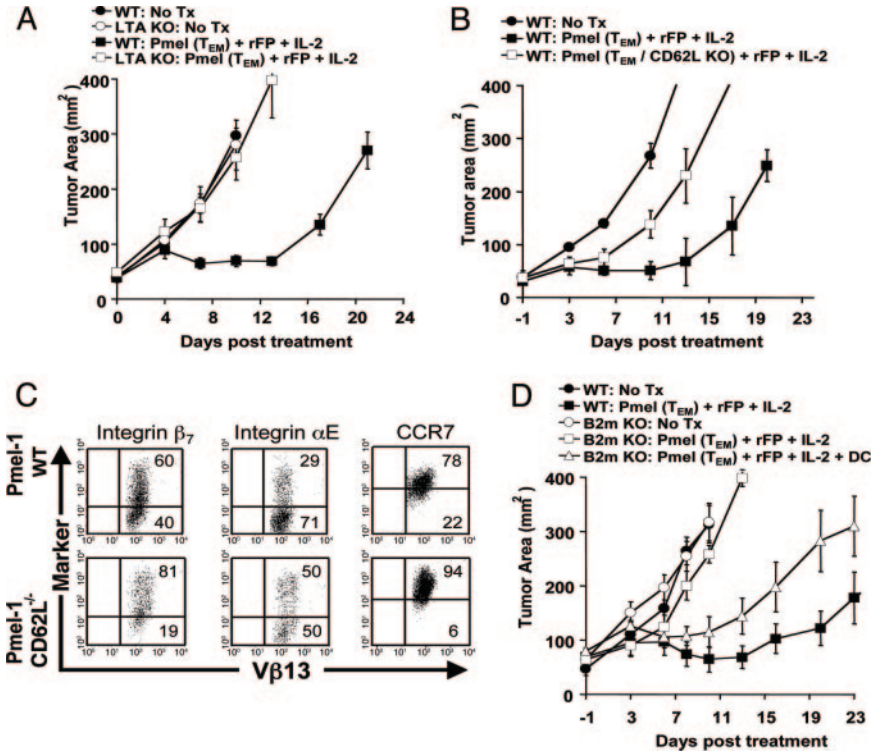

Fig. 1. Trafficking of tumor-reactive $CD8^+$ T cells to 2° lymphoid tissues is required for antitumor treatment. (*A*) WT or $LT\alpha^{-/-}$ mice bearing 9-day s.c. B16 tumors were left untreated as controls (● and ○, respectively) or received 1×10^6 pmel T_{EM}, rFPhgp100 vaccination, and exogenous IL-2 (■ and □, respectively). (*B*) CD62L expression by adoptively transferred tumor-reactive $CD8^+$ T cells is required for optimal antitumor treatment. WT mice bearing 9-day s.c. B16 melanoma tumors were treated with nothing (●), pmel-$CD62L^{-/-}$ cells (□), or age-matched pmel-$CD62L^{+/+}$ cells (■) in combination with rFPhgp100 and exogenous IL-2. (*C*) Redundancy of lymphoid-homing molecules. Splenocytes from pmel-$CD62L^{-/-}$ or age-matched pmel-$CD62L^{+/+}$ controls were stimulated with 1 μM $hgp100_{25-33}$ peptide and cultured under T_{EM} conditions. Cells were cytofluorometrically analyzed on day 6 for the expression of integrin αE, integrin β_7, and CCR7. Numbers represent the percentage of gated cells in each quadrant after gating on propidium iodide-negative and $CD8^+$ lymphocytes. (*D*) Tumor treatment fails in $\beta_2M^{-/-}$ hosts, but can be rescued by cotransfer of BM-derived DCs. WT or $\beta_2M^{-/-}$ mice bearing 9-day B16 tumors were left untreated as controls (● and ○, respectively) or received 1×10^6 T_{EM} pmel, rFPhgp100, and exogenous IL-2 (■ and □, respectively) ± cotransfer of mature BM-derived DCs (▲).

(rFPhgp100) as described (Therion Biologics, Cambridge, MA) (14). Recombinant human IL-2 was administered by i.p. injection twice daily at 36 μg per dose for a total of six doses. Murine bone marrow (BM)-derived dendritic cells (DCs) were generated as described (15). The products of the perpendicular diameters (mean ± SEM) of tumors for tumor growth curves were measured in a blinded fashion with calipers. All experiments were repeated at least twice with similar results.

Microarray and Flow Cytometric Analysis of T_{CM} and T_{EM}. Pmel T_{CM} and T_{EM} were isolated to a purity of >95% by using a no-touch, negative selection CD8-enrichment column (Miltenyl Biotech, Auburn, CA). RNeasy column (Qiagen, Germantown, MD)-purified RNA was indirectly labeled with a single round of linear amplification with Amino Allyl MessageAmp reagents (Ambion, Austin, TX). Labeled samples were combined and hybridized overnight to 22,000-gene long-oligo arrays supplied by the National Cancer Institute (Frederick, MD). Data image files were obtained with a GenePix 4000B scanner (Axon Instruments, Union City, CA) and imported into GENESPRING 6.2 software (Silicon Genetics, Redwood City, CA).

***Ex Vivo* Analysis of Adoptively Transferred Cells.** All antibodies were purchased from BD Pharmingen except anti-human granzyme B-phycoerythrin (GB11) (Caltag, Burlingame, CA). FACScalibur flow cytometer and CELLQUEST software (BD BioSciences, Franklin Lakes, NJ) were used to analyze cells. Adoptively transferred cells in inguinal, axillary, and mesenteric lymph nodes (LNs) were analyzed by cytofluorometry for carboxyfluorescein diacetate succinimidyl ester (CFSE), thy1.1, and CD8. For immunohistochemical staining, inguinal LNs were snap-frozen, stored at −80°C, then sectioned at 7-μm cuts by using cryostat. Sections were Fc-blocked before staining with 10 μg/ml purified anti-PNAd (BD Pharmingen) followed by Cy5-conjugated secondary antibody (Caltag). Sections were mounted with a ProLong Antifade Kit (Molecular Probes) and allowed to stand at room temperature overnight. Images were obtained on a Nikon Eclipse confocal laser-scanning microscope (Bio-Rad). *In vitro* proliferation of pmel T_{EM} and T_{CM} was evaluated by labeling cells with 1 μM CFSE (Molecular Probes) and restimulating with 1 μM $hgp100_{25-33}$-pulsed irradiated splenocytes in complete medium containing 2 ng/ml of recombinant human IL-2.

***In Vitro* Rolling Assay.** Rolling of pmel T_{EM}, pmel T_{CM}, and CD8-enriched naïve cells was determined on 35-mm cell suspension plates (430588) (Corning) coated with GlyCAM-1 (a gift from S. D. Rosen, University of California, San Francisco), E-selectin (R & D Systems), or 1% BSA in PBS, held overnight at 4°C, and blocked with 1% BSA for 1 h at 4°C. Calcein-acetomethyl-labeled (Molecular Probes) T cells were injected at 1.5 dynes per cm^2 into a parallel plate flow chamber (Glycotech, Gaithersburg, MD). Cells were digitally photographed (≈1 image per s) in four to six random fields (each field = 1.18 mm^2) with excitation at 488 nm and emission at 513 nm, and nonmoving and moving cells were differentiated with the IPLAB software program (Scanalytics, Fairfax, VA) and compared by using the Student *t* test.

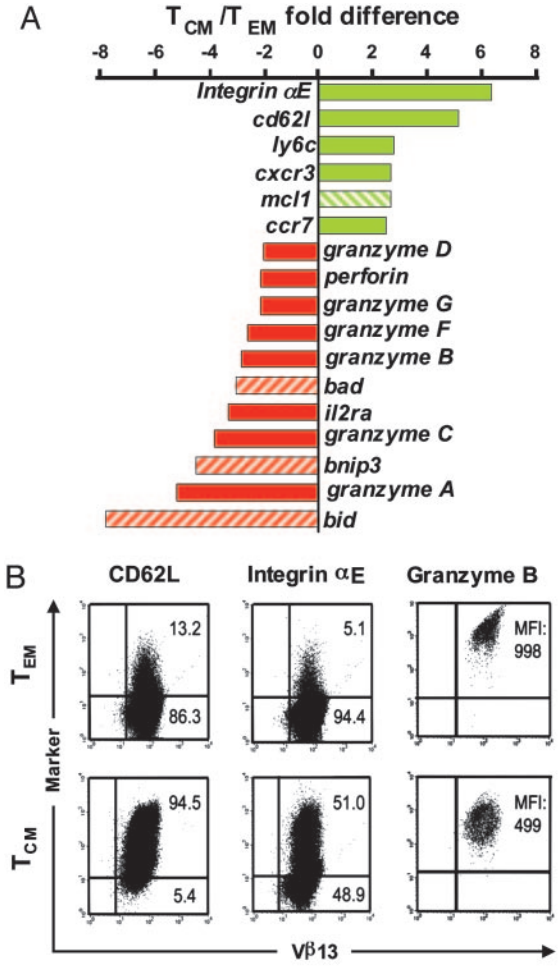

Fig. 2. Gene expression profiling and FACS analysis of self/tumor-reactive $CD8^+$ T_{CM} vs. T_{EM}. (*A*) A selected summary of microarray results. Shown in green are the genes involved in trafficking to 2° lymphoid organs; the hatched green bar indicates a gene (*mcl1*) that has antiapoptotic activity; shown in red are genes involved in effector functions; and hatched red bars indicate proapoptotic genes. (*B*) Cytofluorometric validation of microarray results of pmel T_{CM} and T_{EM}. Surface expression of CD62L and integrin αE are shown with the percentages of $CD8^+$ lymphocytes in each quadrant or the mean fluorescence intensity (MFI) for intracellular granzyme B.

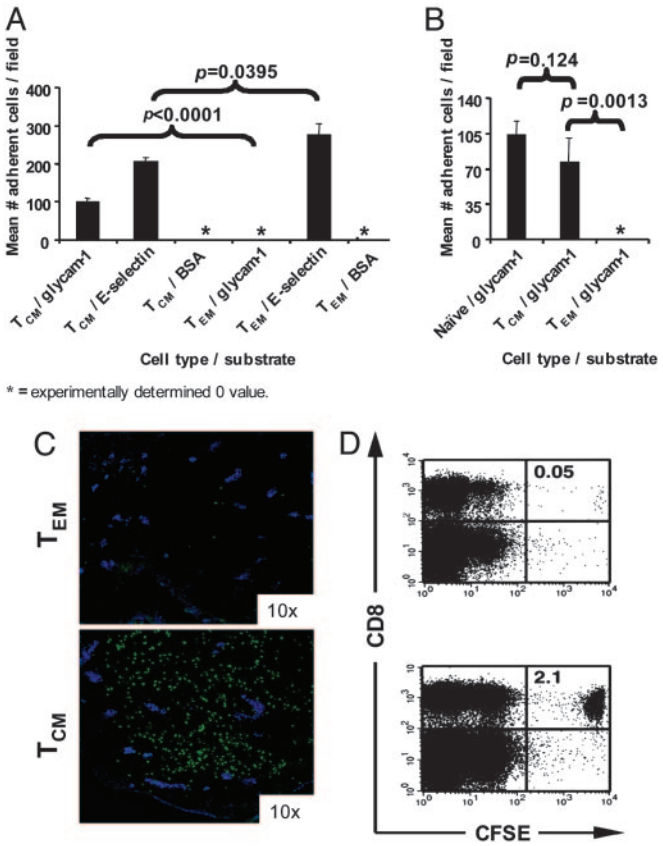

Fig. 3. LN-homing attributes of tumor Ag-specific $CD8^+$ T_{CM} vs. T_{EM}. (*A* and *B*) Pmel T_{CM} but not T_{EM} roll efficiently on substrates coated with glycam-1, a ligand for CD62L. Calcein-acetomethyl-labeled pmel T_{CM}, T_{EM}, or CD8-enriched naïve cells were injected at 1.5 dynes per cm^2 into a parallel plate flow chamber in which the bottom plate was coated with glycam-1, E-selectin, or BSA. After 4 min, rolling cells were photographed (four to six random fields per condition) and counted in a blinded fashion (mean ± SD). (*C* and *D*) *In vivo* LN homing of pmel T_{CM} vs. T_{EM}. CFSE-labeled, pmel-thy1.1 T_{CM} and T_{EM} were adoptively transferred into separate Thy1.2 WT mice, and LNs were extracted 24 h later. (*C*) Cryostat sections of inguinal LNs 24 h after ACT of 4×10^6 CFSE-labeled (green) pmel T_{CM} (*Lower*) or T_{EM} (*Upper*). High endothelial venules were identified by staining for PNAd followed by Cy5-conjugated secondary antibody (blue). (*D*) Cytofluorometric analysis for $CFSE^+CD8^+$ cells from homogenized peripheral LNs and Peyer's patches of recipient mice 24 h after ACT.

Results

Trafficking to 2° Lymphoid Tissues Is Required for Optimal Antitumor Treatment. Altered peptide ligand (14, 15) vaccine-encoded tumor Ag presentation by professional Ag-presenting cells promotes optimal antitumor immunity (16). We therefore hypothesized that trafficking of adoptively transferred cells to 2° lymphoid organs could lead to an enhanced *in vivo* antitumor response. To evaluate the lymphoid trafficking requirements of adoptively transferred pmel cells, we compared the tripartite treatment regimen of cells, rFPhgp100 vaccination, and exogenous IL-2 in tumor-bearing C57BL/6 (WT) and lymphotoxin-$\alpha^{-/-}$ ($LT\alpha^{-/-}$) mice. $LT\alpha^{-/-}$ mice lack peripheral lymphoid structures, including LNs and mucosal Peyer's patches, and possess a disorganized splenic white pulp (17). To provide a treatment window, we intentionally transferred a noncurative dose (1×10^6) of pmel T_{EM}. There was no statistical difference in tumor growth between untreated WT and $LT\alpha^{-/-}$ mice ($P = 0.8550$) (Fig. 1*A*). As previously shown by our group, the combination of pmel T_{EM}, vaccination, and IL-2 caused a pronounced delay in tumor growth in WT mice compared with untreated controls ($P < 0.0001$) (12, 14, 18). By contrast, the antitumor effect was completely abrogated in $LT\alpha^{-/-}$ mice. There was no statistical difference in tumor growth between untreated $LT\alpha^{-/-}$ mice and $LT\alpha^{-/-}$ mice that received cells, vaccine, and IL-2 ($P = 0.6200$). Thus, 2° LNs were required in the tumor-bearing host for optimal tumor treatment.

To determine the influence of L-selectin (CD62L), a critical mediator of lymphocyte homing to 2° LNs (19), we adoptively transferred T_{EM} from pmel-$CD62L^{-/-}$ or age-matched pmel-$CD62L^{+/+}$ controls in combination with vaccine and IL-2 into tumor-bearing WT mice. Although treatment with either T_{EM} pmel-$CD62L^{-/-}$ or pmel-$CD62L^{+/+}$ cells resulted in delayed tumor growth compared with untreated controls ($P = 0.0018$ and < 0.001, respectively), pmel-$CD62L^{+/+}$ cells conferred superior treatment efficacy compared with pmel-$CD62L^{-/-}$ cells ($P = 0.0091$) (Fig. 1*B*). Thus, CD62L was functionally important for antitumor T cell function *in vivo*. Phenotypic analysis revealed, however, that the overexpression of other LN-homing receptors might partially compensate for the lack of CD62L, including integrin β_7, integrin αE, and CCR7 (Fig. 1*C*).

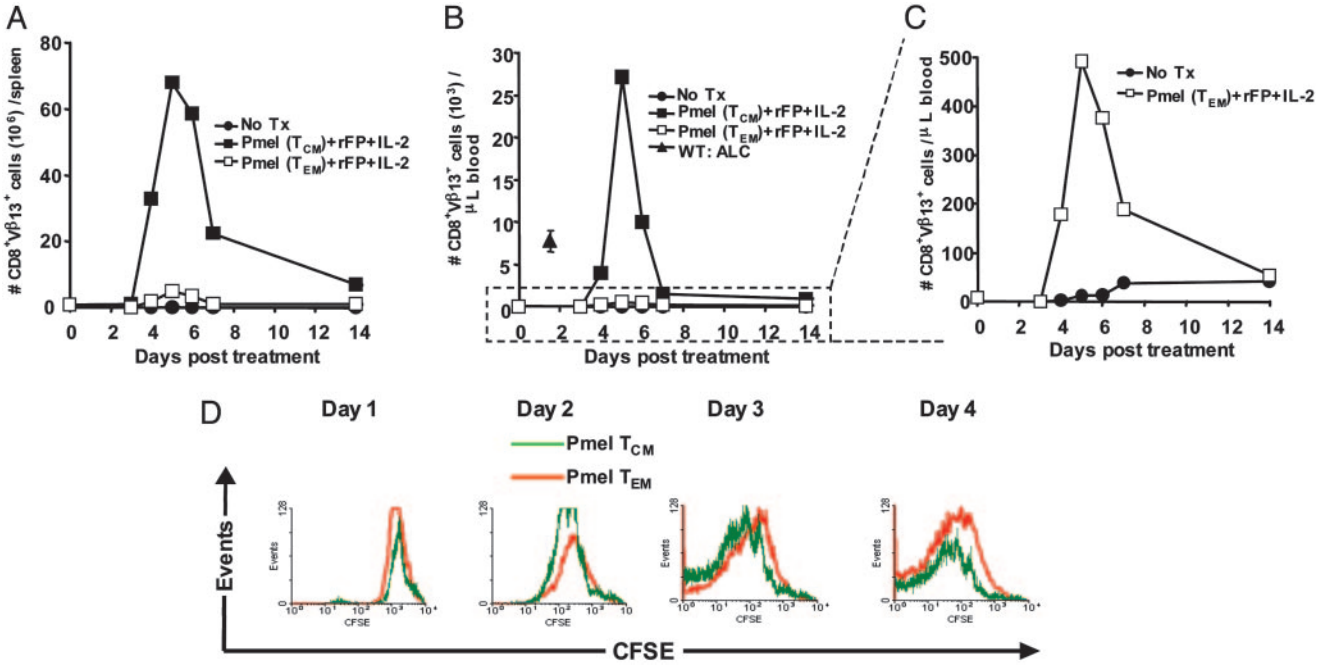

Fig. 4. Enhanced *in vivo* recall response of tumor-Ag-specific $CD8^+$ T_{CM} over T_{EM}. (*A–C*) Sublethally irradiated WT mice bearing 9-day established B16 tumors were left untreated as controls (●) or received the tripartite combination of rFPhgp100, exogenous IL-2, and 1×10^6 pmel T_{CM} (■) or T_{EM} (□). Absolute numbers of adoptively transferred pmel-1 cells (identified by $CD8^+V\beta13^+$ lymphocytes) were enumerated in the spleens or blood of treated animals as a function of time. Each data point represents the average of at least two mice per group. For comparison, the mean absolute lymphocyte count (± SEM) of five nonirradiated tumor-bearing WT mice is shown (▲). (*D*) Comparison of the intrinsic proliferative capacity of restimulated pmel T_{CM} vs. T_{EM}. Pmel-thy1.1 cells expanded under T_{CM} (light lines) or T_{EM} (bold lines) conditions were CFSE-labeled, then restimulated with irradiated WT splenocytes pulsed with $hgp100_{25–33}$ peptide in complete media containing IL-2. CFSE dilution was determined by daily FACS analysis after gating on $CD8^+thy1.1^+$ lymphocytes.

To test whether homing of adoptively transferred pmel-1 cells to LNs facilitated their interaction with resident professional Ag-presenting cells expressing the vaccine-encoded $hgp100_{25–33}$, we compared the treatment efficacy of our tripartite regimen in tumor-bearing WT versus $\beta_2M^{-/-}$ mice. Tumor growth was identical in untreated WT and $\beta_2M^{-/-}$ controls ($P = 0.963$) (Fig. 1*D*). The tripartite regimen of cells, vaccine, and IL-2 was effective at delaying tumor growth in WT mice ($P = 0.0034$) but was not effective in the same experiment in mice incapable of presenting MHC class I-restricted Ags (untreated vs. treated $\beta_2M^{-/-}$ mice $P > 0.05$). This lack of treatment effect could be partially rescued by the cotransfer of β_2M-intact mature BM-derived DCs ($P = 0.009$ vs. no treatment). No rescue was observed when DCs were generated from $\beta_2M^{-/-}$ mice (data not shown). Thus, we determined that trafficking of adoptively transferred tumor-reactive $CD8^+$ T cells to organized 2° lymphoid tissues was necessary for optimal *in vivo* antitumor efficacy in a combined immunotherapy treatment regimen that includes tumor-Ag vaccination.

Gene Expression Profiling of $CD8^+$ T_{CM} vs. T_{EM}. Because trafficking to 2° lymphoid tissues by adoptively transferred pmel cells facilitated their *in vivo* antitumor efficacy, we sought to create T cells with enhanced LN-homing attributes. Naïve, peptide-stimulated $CD8^+$ T cells expanded in the presence of IL-15 give rise to *in vitro* differentiated T_{CM}, whereas IL-2 caused the expansion of T_{EM} that lost the expression of the LN-homing markers CD62L and CCR7 (8, 12, 13). To more fully characterize the attributes of these two cell populations, we performed microarray analysis (GEO accession nos. GSE2578 and GSM49518, www.ncbi.nlm.nih.gov/geo). A total of 476 of the 22,000 genes sampled were differentially expressed between pmel T_{CM} and T_{EM}. Remarkably, genes associated with homing to 2° lymphoid tissues, including *integrin aE*, *cd62l*, *ly6c*, *cxcr3*, and *ccr7*, were among those RNAs overexpressed by pmel T_{CM} compared with T_{EM} (Fig. 2*A*). Additionally, *mcl1*, an antiapoptosis molecule implicated in the maintenance of mature T lymphocytes, was also up-regulated by T_{CM} (20). By contrast, genes associated with effector functions (*granzyme A*, *B*, *C*, *D*, *F*, *G*, *H*, and *perforin*) and proapoptotic signaling (*Bid*, *Bnip3*, and *Bad*) were among the most highly overexpressed in T_{EM} (Fig. 2*A*). Microarray results for CD62L, integrin αE, and intracellular granzyme B on pmel T_{CM} and T_{EM} were validated by cytofluorometry (Fig. 2*B*). Consistent with previously published FACS results, CD62L expression was notably higher in pmel T_{CM} than in T_{EM} (12). Integrins αE (Fig. 2*B*) and β_7 (data not shown) were two additional lymphoid-homing molecules that were overexpressed on pmel T_{CM}. Conversely, pmel T_{EM} exhibited a higher level of granzyme B expression compared with pmel T_{CM} (mean fluorescence intensity = 998 and 499, respectively). These data indicated that some of the most pronounced gene and protein expression differences between pmel T_{CM} and T_{EM} relate to the capacity to home to LNs and the acquisition of effector functions, respectively.

***In Vitro* and *in Vivo* LN-Homing Attributes of Tumor Ag-Specific T_{CM} and T_{EM}.** To determine whether the gene and protein expression profiling results of pmel T_{CM} and T_{EM} were reflected in functional difference in tissue homing behavior, we evaluated the *in vitro* rolling of pmel T_{CM} and T_{EM} under physiologic shear flow conditions. We used substrates coated with glycam-1, a ligand for CD62L expressed in the high endothelial venules of peripheral LNs (19). Neither population of cells rolled on substrates coated with BSA, an irrelevant protein control (Fig. 3*A*). Both pmel T_{CM} and CD8-enriched naïve pmel-1 cells, a lymphocyte population with optimal LN-homing attributes, rolled on glycam-1, whereas pmel T_{EM} did not ($P < 0.01$) (Fig. 3 *A* and *B*). T_{EM} reportedly display a characteristic pattern of surface chemokine and adhe-

sion molecules required for homing to inflamed peripheral tissues (7). To test this capacity, we assayed rolling of *in vitro*-generated pmel T_{CM} and T_{EM} on substrates coated with E-selectin, a leukocyte adhesion molecule expressed on endothelial cells at inflammatory sites. Both cell types rolled on this substrate (Fig. 3*A*); however, a greater number of pmel T_{EM} compared with T_{CM} was found on E-selectin ($P < 0.05$). Therefore, pmel T_{EM} possessed *in vitro* properties consistent with an enhanced propensity to traffic to inflamed peripheral tissues, whereas pmel T_{CM} displayed enhanced LN-homing attributes.

We next investigated the *in vivo* LN-homing properties of these two cell populations. We adoptively transferred CFSE-labeled pmel-thy1.1 T_{CM} and T_{EM} into thy1.2 C57BL/6 hosts. Twenty-four hours after ACT, we extracted peripheral LNs of recipient mice for immunohistochemical staining and FACS analysis. Grossly, immunohistochemical staining of inguinal LNs 24 h after ACT revealed a pronounced accumulation of adoptively transferred CFSE-labeled cells in animals that received pmel T_{CM}, but not T_{EM} (Fig. 3*C*). Cytofluorometric analyses of peripheral LNs was performed to quantitate these results, and multiple independent experiments confirmed that there was between 20 and 40 times the number of $CFSE^+CD8^+$ cells present in lymphoid tissues in animals that received pmel T_{CM} compared with T_{EM} (Fig. 3*D*). These results were not caused by differential CFSE dilution by pmel T_{EM} because similar results were obtained by analysis for $CD8^+$ $Thy1.1^+$ cells (data not shown). These data demonstrated that gene expression profiling of pmel-1 cells expanded under T_{CM} and T_{EM} conditions accurately depicted the *in vitro* and *in vivo* LN-homing attributes of these two populations of tumor-reactive $CD8^+$ T cells.

Enhanced *in Vivo* Recall Response and Tumor Treatment of T_{CM} Compared with T_{EM}. To determine the functionality of T_{CM} and T_{EM} *in vivo*, we adoptively transferred *in vitro*-differentiated pmel subsets into sublethally irradiated tumor-bearing WT mice in combination with vaccine and IL-2. The *in vivo* recall response of these two cell populations (as assessed by the enumeration of the absolute numbers of adoptively transferred pmel-1 cells in the spleens and blood of treated animals) revealed that there was a marked expansion of adoptively transferred T_{CM} and T_{EM}, peaking in both groups ≈5 days after transfer (Fig. 4*A*). Importantly, the magnitude of the response in the spleens of mice that received T_{CM} was strikingly greater, peaking at levels four to 14 times higher than T_{EM} in individual experiments. These results were not caused simply by the differential accumulation of T_{CM} in the spleen because an analogous proliferation pattern was also observed in the blood, a nonlymphoid tissue (Fig. 4 *B* and *C*). Indeed, animals that received T_{CM} experienced a true tumor-reactive $CD8^+$ T cell lymphocytosis that was more than three times the absolute lymphocyte count of WT mice, a phenomenon not observed with T_{EM}. The *in vivo* results were not caused merely by intrinsic differences in proliferative capacity of T_{CM} over T_{EM}, because there was a similar rate of CFSE dilution in these two cell populations in an *ex vivo* assay (Fig. 4*D*).

Pronounced lymphocytosis in melanoma patients treated with ACT after lymphodepletion has been correlated with antitumor efficacy (5). To determine whether the lymphocytosis observed in mice treated with T_{CM} correlated with the antitumor effect, we treated sublethally irradiated mice bearing 9-day established B16 melanoma with ACT at a dose of pmel cells (1×10^6) previously established to be noncurative when T_{EM} are used in combination with vaccine and IL-2. As previously shown, the suboptimal tripartite regimen using pmel T_{EM} caused a pronounced delay without cures in tumor growth compared with untreated controls ($P = 0.0069$) (Fig. 5*A*). Treatment with T_{CM} delayed tumor growth significantly compared with both untreated controls ($P < 0.0001$) and T_{EM}-treated mice ($P = 0.0014$). In addition, a T_{CM}-based regimen caused improved survival ($P < 0.002$) (Fig. 5*B*). Thus, ACT of a T_{CM} population, in combination with tumor-Ag vaccination and exogenous IL-2, produced a more robust and therapeutically significant *in vivo* recall response compared with T_{EM}.

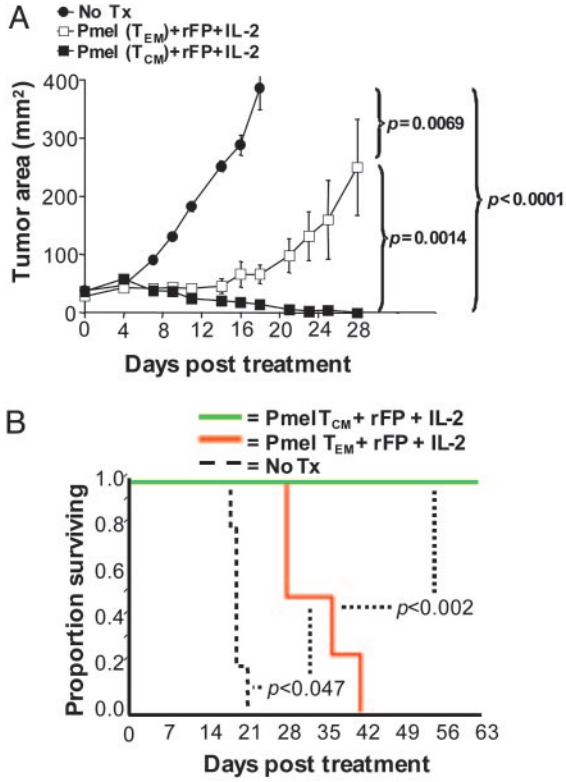

Fig. 5. Tumor-reactive $CD8^+$ T_{CM} are superior to T_{EM} in the treatment of B16 melanoma. (*A*) Sublethally irradiated (5 Gy) WT mice bearing 9-day B16 tumors were left untreated as controls (●) or received rFPhgp100 vaccination, exogenous IL-2, and either pmel T_{CM} (■) or T_{EM} (□). (*B*) Enhanced tumor regression in mice receiving pmel T_{CM} correlated with statistically prolonged animal survival, compared with mice receiving T_{EM}.

Discussion

Recent human trials for the adoptive immunotherapy of cancer have demonstrated a statistical correlation between the persistence of transferred tumor-reactive T cells and the therapeutic response that could objectively be achieved in ≈50% of the patients treated by using cells with T_{EM} or effector T cell phenotype (21). Although preliminary work using viral Ags has suggested that T_{CM} are superior mediators of a recall response to Ag challenge (8, 9), some have recently called these findings into question (10). In the present studies, we evaluated the role of T_{EM} and T_{CM} populations as mediators of an immune response to an established disease. We found that Ag-specific T_{CM} mounted a heightened *in vivo* recall response compared with T_{EM}, consistent with other reports (9, 22). Importantly, this enhanced response by T_{CM} was associated with the complete eradication of a large, established B16 melanoma. As seen in other models, T_{EM} can generate a 2° response but the relative efficiency of this response was less than that of T_{CM} on a per-cell basis (9, 22).

Although T_{CM} and T_{EM} have been subdivided on the basis of their relative expression of lymphoid-homing molecules (7, 11), these two populations also possess other unique attributes. For example, T_{EM} have been shown to develop effector functions more rapidly than T_{CM} (7, 8). By contrast, T_{CM} are able to release significant amounts of helper cytokines, such as IL-2 (7, 9, 12).

In our own analysis of the differences between T_{CM} and T_{EM} by using oligo microarrays, we found that expression of genes associated with lymphoid homing were among the most highly overexpressed by T_{CM}. The critical importance of homing to 2° LNs by adoptively transferred tumor-reactive T cells was established by experiments in which tumor therapy was completely abrogated in host mice with absent peripheral lymphoid tissues and a disrupted splenic structure. Further evidence that trafficking to LNs is required was provided by using tumor-reactive $CD8^+$ T cells genetically deficient in CD62L.

T cell homing to 2° LNs was required to facilitate interaction with virally infected BM-derived Ag-presenting cells, as evidenced by the absence of tumor treatment in $\beta_2M^{-/-}$ hosts and their rescue by cotransfer of WT BM-derived DCs. It is likely that the enhanced *in vivo* proliferative response of T_{CM} was the result of increased access to vaccine-encoded Ag-expression in 2° LNs as both T_{CM} and T_{EM} exhibited similar intrinsic proliferative responses when Ag levels were normalized *in vitro*. These results indicated that, in addition to prevention, T_{CM} can be a superior mediator of a therapeutic response, and this effect highly depended on the cells' homing to lymphoid tissues.

The approach of targeting T cell trafficking to LNs provides an alternative to attempts to cause the initial trafficking of adoptively transferred immune cells to tumors directly (23). These efforts have included the insertion of genes encoding chemokine receptors into lymphocytes to enhance their recruitment to tumor sites (24) and the genetic modification of the tumor microenvironment itself through the forced expression of LIGHT, a tumor necrosis factor superfamily member used to enhance the recruitment, retention, and activation of T cells (25). Thus, the alternative and perhaps complementary approach described here is the use of concomitant tumor-Ag vaccination that induces a massive clonal expansion and subsequent infiltration of numerous tissues by antitumor T cells (18) that obviates the requirement for immediate and specific targeting of the tumor site.

These results have implications for the design of human adoptive immunotherapy trials. In most currently used protocols, the cells generated for ACT acquire effector T cell/T_{EM} phenotypic and functional attributes before transfer (4). Our data suggest that ACT of these populations may be suboptimal; although response rates approaching 50% can now be obtained with the transfer of very large numbers (up to 1×10^{11}) of *ex vivo*-expanded T cells (5). The transfer of a more efficient antitumor T_{CM} population might increase the proliferation and persistence of cells upon adoptive transfer *in vivo*. Our findings may have significant implications for the selection and the generation of optimal antitumor T cells for ACT in cancer patients. The generation of T_{CM} may be accomplished by altering duration and nature of T cell culture conditions in human clinical trials.

C.A.K. dedicates this manuscript to Grandma Anne Anderson and her personal battle with cancer. We thank D. Surman, P. J. Spiess, Z. Yu, and Y. Lou for technical assistance.

1. Dudley, M. E. & Rosenberg, S. A. (2003) *Nat. Rev. Cancer* **3,** 666–675.
2. Klebanoff, C. A., Khong, H. T., Antony, P. A., Palmer, D. C. & Restifo, N. P. (2005) *Trends Immunol.* **26,** 111–117.
3. Yee, C., Thompson, J. A., Byrd, D., Riddell, S. R., Roche, P., Celis, E. & Greenberg, P. D. (2002) *Proc. Natl. Acad. Sci. USA* **99,** 16168–16173.
4. Powell, D. J., Jr., Dudley, M. E., Robbins, P. F. & Rosenberg, S. A. (2005) *Blood* **105,** 241–250.
5. Dudley, M. E., Wunderlich, J. R., Yang, J. C., Sherry, R. M., Topalian, S. L., Restifo, N. P., Royal, R. E., Kammula, U., White, D. E., Mavroukakis, S. A., *et al.* (2005) *J. Clin. Oncol.* **23,** 2346–2357.
6. Kaech, S. M., Wherry, E. J. & Ahmed, R. (2002) *Nat. Rev. Immunol.* **2,** 251–262.
7. Sallusto, F., Geginat, J. & Lanzavecchia, A. (2004) *Annu. Rev. Immunol.* **22,** 745–763.
8. Manjunath, N., Shankar, P., Wan, J., Weninger, W., Crowley, M. A., Hieshima, K., Springer, T. A., Fan, X., Shen, H., Lieberman, J., *et al.* (2001) *J. Clin. Invest.* **108,** 871–878.
9. Wherry, E. J., Teichgraber, V., Becker, T. C., Masopust, D., Kaech, S. M., Antia, R., Von Andrian, U. H. & Ahmed, R. (2003) *Nat. Immunol.* **4,** 225–234.
10. Roberts, A. D. & Woodland, D. L. (2004) *J. Immunol.* **172,** 6533–6537.
11. Weninger, W., Crowley, M. A., Manjunath, N. & Von Andrian, U. H. (2001) *J. Exp. Med.* **194,** 953–966.
12. Klebanoff, C. A., Finkelstein, S. E., Surman, D. R., Lichtman, M. K., Gattinoni, L., Theoret, M. R., Grewal, N., Spiess, P. J., Antony, P. A., Palmer, D. C., *et al.* (2004) *Proc. Natl. Acad. Sci. USA* **101,** 1969–1974.
13. Miyahara, N., Swanson, B. J., Takeda, K., Taube, C., Miyahara, S., Kodama, T., Dakhama, A., Ott, V. L. & Gelfand, E. W. (2004) *Nat. Med.* **10,** 865–869.
14. Overwijk, W. W., Theoret, M. R., Finkelstein, S. E., Surman, D. R., de Jong, L. A., Vyth-Dreese, F. A., Dellemijn, T. A., Antony, P. A., Spiess, P. J., Palmer, D. C., *et al.* (2003) *J. Exp. Med.* **198,** 569–580.
15. Lou, Y., Wang, G., Lizee, G., Kim, G. J., Finkelstein, S. E., Feng, C., Restifo, N. P. & Hwu, P. (2004) *Cancer Res.* **64,** 6783–6790.
16. Bronte, V., Carroll, M. W., Goletz, T. J., Wang, M., Overwijk, W. W., Marincola, F., Rosenberg, S. A., Moss, B. & Restifo, N. P. (1997) *Proc. Natl. Acad. Sci. USA* **94,** 3183–3188.
17. De Togni, P., Goellner, J., Ruddle, N. H., Streeter, P. R., Fick, A., Mariathasan, S., Smith, S. C., Carlson, R., Shornick, L. P., Strauss-Schoenberger, J., *et al.* (1994) *Science* **264,** 703–707.
18. Palmer, D. C., Balasubramaniam, S., Hanada, K., Wrzesinski, C., Yu, Z., Farid, S., Theoret, M. R., Hwang, L. N., Klebanoff, C. A., Gattinoni, L., *et al.* (2004) *J. Immunol.* **173,** 7209–7216.
19. Rosen, S. D. (2004) *Annu. Rev. Immunol.* **22,** 129–156.
20. Opferman, J. T., Letai, A., Beard, C., Sorcinelli, M. D., Ong, C. C. & Korsmeyer, S. J. (2003) *Nature* **426,** 671–676.
21. Robbins, P. F., Dudley, M. E., Wunderlich, J., El Gamil, M., Li, Y. F., Zhou, J., Huang, J., Powell, D. J., Jr. & Rosenberg, S. A. (2004) *J. Immunol.* **173,** 7125–7130.
22. Bouneaud, C., Garcia, Z., Kourilsky, P. & Pannetier, C. (2005) *J. Exp. Med.* **201,** 579–590.
23. Ho, W. Y., Blattman, J. N., Dossett, M. L., Yee, C. & Greenberg, P. D. (2003) *Cancer Cell* **3,** 431–437.
24. Kershaw, M. H., Wang, G., Westwood, J. A., Pachynski, R. K., Tiffany, H. L., Marincola, F. M., Wang, E., Young, H. A., Murphy, P. M. & Hwu, P. (2002) *Hum. Gene Ther.* **13,** 1971–1980.
25. Yu, P., Lee, Y., Liu, W., Chin, R. K., Wang, J., Wang, Y., Schietinger, A., Philip, M., Schreiber, H. & Fu, Y. X. (2004) *Nat. Immunol.* **5,** 141–149.
26. Gattinoni, L., Klebanoff, C. A., Palmer, D. C., Wrzesinski, C., Kerstann, K., Yu, Z., Finkelstein, S. E., Theoret, M. R., Rosenberg, S. A. & Restifo, N. P. (2005) *J. Clin. Invest.* **115,** 1616–1626.